SINGLE-HEADED BINDING OF A SPIN-LABELED-HMM-ADP COMPLEX TO F-ACTIN

Saturation Transfer Electron Paramagnetic Resonance and Sedimentation Studies

BARBARA A. MANUCK, JOHN C. SEIDEL, AND JOHN GERGELY
Department of Muscle Research, Boston Biomedical Research Institute; Department of Neurology, Massachusetts General Hospital; and Departments of Biological Chemistry and Neurology, Harvard Medical School, Boston, Massachusetts 02114

SUMMARY The interaction of actin and spin-labeled heavy meromyosin (MSL-HMM) was studied in the presence and absence of adenosine diphosphate or 5'-adenyl-yl-imidodiphosphate (AMPPNP) to determine the contributions of single and double-headed binding. The extent of single-headed binding to actin was deduced from a comparison of the fraction of immobilized *heads* (f_i) with the fraction of bound *molecules* (f_s) determined by saturation-transfer EPR (ST-EPR) and sedimentation, respectively. The ST-EPR measurements depend on the reduced motion of the spin label rigidly bound to the HMM heads upon the interaction of the latter with actin. During titration of acto-MSL-HMM with nucleotide, we measured changes in f_i and f_s brought about by dissociation of MSL-HMM from actin. On titration with ADP, f_s changed very little, remaining above 0.8, while f_i decreased to ~0.5 at 10mM ADP, a result consistent with extensive single-headed binding of MSL-HMM to actin. On titration with AMPPNP, single-headed binding was not detected; viz., f_i and f_s decreased in parallel. It was not necessary to postulate a nucleotide induced state of the bound heads, differing in motional properties from that of rigor heads, to account for the results.

INTRODUCTION

Saturation transfer electron paramagnetic resonance (ST-EPR) studies using spin labels rigidly attached to myosin heads have shown that the rotational motion of the heads is greatly reduced upon attachment to actin—the correlation time changes from ~10 μs to ~1 ms—in actomyosin, myofibrils in rigor and glycerol extracted fibers (1–5). Although the most widely accepted molecular model of muscle contraction envisages a rotation of the attached myosin heads about an axis perpendicular to the actin filament, ST-EPR and fluorescence studies on myofibrils and muscle fibers in the presence of ATP, under conditions of activation of the ATPase activity of myosin, have failed to reveal any state different from either rigor or detached heads (4, 6). Neither have time resolved x-ray studies on living fibers, although showing clear changes in the diffraction pattern that slightly precede tension development on the millisecond timescale, yielded evidence of actual rotation of the heads (7, 8). The studies of Burghardt et al. (9), however, using a rhodamine label suggest that, in the presence of ADP or under conditions simulating contraction, crossbridges attach with an angular attitude differing from that in rigor.

The results of our previous EPR studies with ATP analogues under conditions leading to partial dissociation that induced increased rotational mobility of the spin-labeled myosin heads in myofibrils were interpreted in terms of two populations of heads—attached and detached—each having distinct rotational properties regardless whether a nucleotide or PP_i was actually bound (5). The present studies were undertaken to examine the motional properties of attached heads in the acto-MSL-HMM system in the presence of ADP or the non-hydrolyzable ATP analogue AMPPNP.[1] We wished to obtain information on the possible existence of a nucleotide induced state, distinct from rigor or detached states, and to throw some light on the question of single-headed vs. double-headed attachment of myosin to actin. The latter point is of interest since most schemes of myosin-actin interaction treat myosin without regard to its two-headed nature. In fact, some binding studies on acto-HMM in vitro provide evidence for single-headed binding in the presence of nucleotides (10–12). Our results are consistent with a binding mechanism in which spin-labeled heavy meromyosin in the presence of ADP, binds to actin by one head, which is immobilized on a submillisecond time scale

[1] *Abbreviations used in this paper:* εADP, 1-ethenoadenosine-5'-diphosphate; Ad_2P_5, diadenosine pentaphosphate; AMPPNP, 5'-adenylyl imidodiphosphate; EGTA, ethylene glycol bis(β-aminoethyl ether)-N,N,N',N'-tetraacetic acid; HMM, heavy meromyosin; MOPS, 4-morpholinopropane sulfonic acid; MSL, N-(1-oxyl-2,2,6,6,-tetramethyl-4-piperidinyl) maleimide; S1, subfragment-1; ST-EPR, saturation transfer electron paramagnetic resonance.

while the free head shows a rate of motion approaching that of synthetic myosin filaments (1, 13–15). It was not necessary to postulate a nucleotide induced state of the bound head, differing in motional properties from that in rigor, to account for the results.

METHODS

Preparation and Spin-labeling of Myosin Fragments

Myosin from rabbit skeletal muscle was prepared as described previously (16). Before use the ammonium sulfate-precipitated pellet was dissolved in a solution containing 0.5 M KCl, 10 mM MOPS and 0.1 mM EDTA, pH 7 and dialyzed exhaustively against the same solution. The solution of myosin was then centrifuged at 100,000 *g* for 60 min to remove any insoluble protein. All protein preparations were carried out at 0–4°C and all buffers contained 1 mM NaN_3.

Labeling with the spin label 4-maleimido-2,2,6,6-tetramethyl-piperidinooxyl (MSL) at the SH1 thiols of myosin was carried out according to Thomas et al. (3) in low ionic strength buffer (0.05 M KCl, 1 mM EDTA, 10 mM MOPS, pH 7). The labeled myosin in suspension was washed three times by centrifugation at 100,000 *g* for 30 min followed by resuspension in low ionic strength buffer. For preparation of spin-labeled heavy meromyosin (MSL-HMM) or subfragment-1 (MSL-S1), digestion of spin-labeled myosin with chymotrypsin was carried out according to the procedure of Weeds and Pope (17) in a solution containing 0.5 M KCl, 0.1 mM $MgCl_2$, 10 mM MOPS, pH 7, to prepare HMM or in 0.12 M KCl, 1 mM EDTA, 10 mM MOPS, pH 7, to prepare S1. The digests were dialyzed against 0.04 M KCl, 10 mM MOPS, pH 7 overnight to precipitate the insoluble proteins, including undigested myosin, which were then removed by centrifugation. To remove weakly immobilized EPR spectral components, solutions of MSL-S1 or MSL-HMM were treated with 50 mM $K_3Fe(CN)_6$ for 10–12 h (18); excess reagent was removed by dialysis against a solution containing 0.1 M KCl and 10 mM MOPS, pH 7. Purification was achieved by precipitation with 50% saturated $(NH_4)_2SO_4$ followed by centrifugation at 100,000 *g*; four to five pellets, each containing 30 mg of protein were obtained and stored at −80°C. Typically, 1.0–1.2 labels per head were present in the final preparations of MSL-S1 or MSL-HMM.

Solutions of labeled protein were prepared by dialyzing an $(NH_4)_2SO_4$ pellet against 0.1 M KCl, 10 mM MOPS, pH 7 for 24–30 h and clarified by centrifugation for 30 min at 100,000 *g*. The concentrations of MSL-S1 and MSL-HMM were determined using A_{280} (1 mg/ml, 1 cm) = 0.77, M_r = 115,000; and A_{280} = 0.65, M_r = 362,000, respectively (19).

Actin was prepared from an acetone powder of rabbit skeletal muscle (19) and stored in pellets obtained by sedimentation for 3 h at 100,000 *g* of G-actin polymerized with 0.1 M KCl, 1.0 mM $MgCl_2$. For the binding studies, a portion of a pellet was depolymerized by gentle homogenization in a solution of 2 mM Tris, 0.2 mM ATP, pH 7.5 followed by repolymerization by the addition of KCl and $MgCl_2$ to final concentrations of 0.1 M and 1.0 mM, respectively. The concentration of the stock solution of actin was determined spectrophotometrically in the G form prior to the final polymerization step using A_{290} (1 mg/ml, 1 cm) = 0.63, M_r = 42,000 (19).

Titration of Acto-MSL-HMM, Acto-MSL-S1 with AMPPNP or ADP

MSL-HMM or MSL-S1 and actin were mixed in a solution (final volume 0.75 ml) containing 0.2 M KCl, 50 mM MOPS, 5 mM $MgCl_2$, 20 μM diadenine pentaphosphate (Ad_2P_5), 1 mM NaN_3, pH 7 and nucleotide (ADP or AMPPNP) at a concentration of 0 to 10 mM. After stirring with a small magnetic bar for 10 min, each solution was allowed to stand for 30 min before the ST-EPR spectrum was recorded. An aliquot of each sample was then centrifuged as described below to determine the fraction of MSL-HMM or MSL-S1 bound to F-actin. A separate mixture of proteins was prepared for each concentration of nucleotide.

EPR Spectroscopy

Conventional EPR (V_1) and saturation transfer EPR spectra (V_2') were obtained according to Thomas et al. (3, 20) on a Varian E-109E spectrometer operating at 9.5 GHz, with sweep times of 8 min for conventional and 60 min for saturation transfer EPR. All samples were in a large flat quartz cell, without a Dewar insert, at the ambient cavity temperature of 27°C. The concentration of nitroxide labels was determined by double integration of the V_1 spectra with a Nicolet computer interfaced to the spectrometer. The spin label has been shown (3) to be rigidly attached to MSL-S1 or the head region of MSL-HMM so that all spectra obtained reflect motion of the proteins themselves rather than that of the label relative to the protein. Intensity measurements in ST-EPR spectra were made at the two low field positions L'' and L (Fig. 1), whose ratio, L''/L, is sensitive to the rate of motion of the protein (20). L and L'' were measured at the magnetic fields described by Thomas et al. (20).

Estimation by Sedimentation of MSL-HMM Bound to Actin

Approximately 0.4 ml of each sample was centrifuged for 30 min in a Beckman Airfuge at 100,000 *g*, 26–27°. Actin and MSL-HMM bound to actin by one or both heads were sedimented while unbound MSL-HMM remained in the supernatant. The time of centrifugation was chosen to sediment at least 98% of the acto-MSL-HMM and to prevent detectable sedimentation of free MSL-HMM. The concentration of free MSL-HMM was determined from the double integral of the V_1 spectrum of the

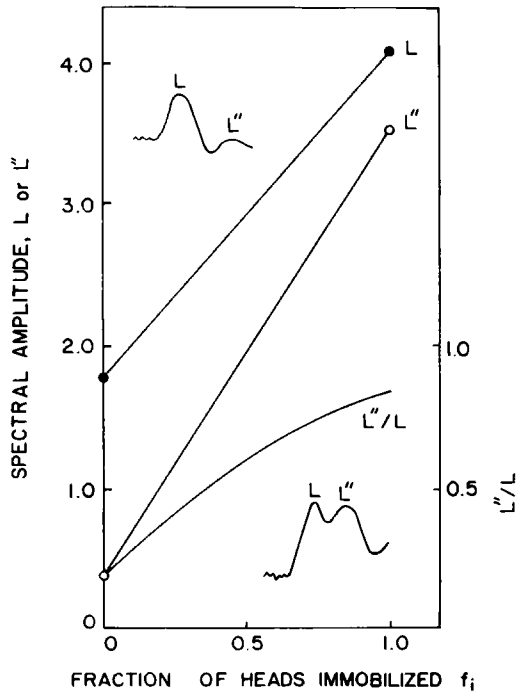

FIGURE 1 Relationship between L''/L and the fraction of immobilized MSL-S1. The insets show the low field region of the ST-EPR spectrum of MSL-S1 in the absence (*upper inset*) or presence (*lower inset*) of 60 μM actin. Spectra of MSL-HMM under these conditions are similar. Spectra were obtained from solutions of MSL-S1 (17 μM) in 0.2 M KCl, 50 mM MOPS, 5 mM $MgCl_2$, 20 μM Ad_2P_5, 1 mM NaN_3, pH 7 at a temperature of 27°C.

supernatant yielding

$$f_s = (\text{total MSL-HMM} - \text{free MSL-HMM in supernatant})/\text{total MSL-HMM},$$

where f_s is the fraction of MSL-HMM molecules bound to actin. The fraction of bound MSL-S1 was determined in the same way.

Estimation by ST-EPR of Heads Immobilized by Actin

A calibration curve (Fig. 1) relating L''/L—L and L'' (20) being the amplitudes of the two low field spectral peaks—to the fraction (f_i) of MSL-S1 immobilized by binding to actin was constructed as described previously for myofibrils (5). L_m and L''_m were obtained from a spectrum of free MSL-S1 in the absence of actin ($f_i = 0$), and L_i and L_i'' from a spectrum of acto-MLS-S1, at the same concentration of MSL-S1, where all of the MSL-S1 is immobilized by binding to actin ($f_i = 1$). The calibration curve for MSL-HMM was constructed in the same way except that values of L and L'' for free and immobilized heads were obtained from spectra of MSL-HMM or acto-MSL-HMM, respectively. In the case of MSL-HMM, f_i is the fraction of immobilized heads. A separate calibration curve was constructed for each titration because of a variation of 10% in the values of L and L'' for different MSL-HMM or MSL-S1 preparations. The calibration curves were used to estimate f_i at each concentration of nucleotide in the titrations of acto-MSL-HMM or acto-MSL-S1 in the initial sample, assuming that nucleotide binding to either a detached or attached head does not change the motional parameters of the label (cf. reference 5).

Determination of the Binding Constant of ADP-MSL-S1 to Actin

MSL-S1, at a final concentration up to 40 μM, was added to a solution containing 0.2 M KCl, 50 mM MOPS, 5 mM $MgCl_2$, 20 μM Ad_2P_5, 3 mM ADP and 10 μM actin, pH 7. The solution was stirred for 10 minutes and then centrifuged for 30 min at 100,000 g to sediment the actin-bound ADP-MSL-S1. The concentration of the ADP-MSL-S1 remaining in the supernatant was determined from the conventional EPR spectrum by double integration. A separate mixture of proteins was prepared at each concentration of MSL-S1.

Titration of MSL-HMM with ϵADP

MSL-HMM was titrated with a fluorescent analogue of ADP (ϵADP, 1-ethenoadenosine-5'-diphosphate) in 0.2 M KCl, 5 mM $MgCl_2$, 50 mM MOPS, 20 μM Ad_2P_5, pH 7. Acrylamide was present at 0.1 M to quench the fluorescence of free ϵADP without affecting ϵADP bound to MSL-HMM (21). The fluorescence intensity was measured as a function of total [ϵADP] in solutions with (F) and without (F_0) MSL-HMM. The concentration of bound ϵADP is

$$c_b = (F - F_0)/(F_b - F_f),$$

where F_b is the molar fluorescence intensity of bound ϵADP in arbitrary units determined from the titration of ϵADP with excess MSL-HMM; F_f is the molar fluorescence of the ϵADP under the same experimental conditions. Fluorescence spectra were obtained with $\lambda_{ex} = 320$ nm and $\lambda_{em} = 405$ nm using a Perkin-Elmer MPF-4 fluorometer. At the completion of the titration, chymotrypsin was added at a ratio of 1:200 and the fluorescence was monitored for 90 min. During this time there was no change in fluorescence while gel electrophoresis in sodium dodecyl sulfate showed the disappearance of MSL-HMM with the formation of MSL-S1.

RESULTS

Titration of Acto-MSL-HMM or Acto-MSL-S1 with AMPPNP and ADP

To compare the fraction of immobilized heads (f_i) with the fraction of bound molecules (f_s), samples of acto-MSL-HMM were subjected to ST-EPR and sedimentation followed by conventional EPR of the supernatant at each concentration of nucleotide (see Methods). On titration with AMPPNP, f_i determined by ST-EPR, and f_s decreased in parallel (Fig. 2 *A*), as would be expected if all the bound MSL-HMM were attached by both heads. The fraction of bound MSL-HMM decreased to 0.1–0.2 at 10 mM AMPPNP indicating dissociation of essentially all the MSL-HMM.

On titration with ADP, the two parameters did not change in parallel. The fraction that sedimented with actin changed very little with increasing ADP concentration, remaining above 0.8 even at saturating concentrations of ADP, while the fraction of immobilized heads decreased to ~0.5 (Fig. 2 *B*). This suggests either that some of the bound heads had more rapid motion than those in rigor or that most of the bound MSL-HMM was attached to actin by only one head.

To distinguish between these two possibilities the same titrations were performed with solutions of acto-MSL-S1. Titration with either ADP or AMPPNP produced a parallel decrease in f_i and f_s (Figs. 3, 4). Titration with AMPPNP produced a maximum dissociation of 90% in agreement with Greene and Eisenberg (22) while ADP dissociated only 20% of the complexes. These results indicate that the motion of attached heads in the presence of ligand is the same as that of rigor heads and favors interpretation of the MSL-HMM data in terms of single-headed attachment (for details see Discussion).

Computer Modeling

The scheme in Fig. 5 *A* was used to model the EPR and sedimentation data (Fig. 2 *A*, *B*). MSL-HMM can exist as a free moiety or in complexes containing one or two nucleotides, any of which can be bound to actin. An equilibrium constant (K'_M, $B3$, etc.; Fig. 5 *A*) is associated with each transition and there is a cumulative formation constant ($K_{A_iML_j}$ where i and j equal 0, 1, or 2), which is the product of the equilibrium constants along a path leading from free MSL-HMM to the complex. With each set of cumulative constants the program calculates the fraction of molecules bound (f_{scalc}) and the fraction of heads bound (f_{icalc}). To fit the data, a maximum of three of the cumulative formation constants were varied by subroutine MINPAK (Argonne National Laboratory) using the Levenberg-Marquardt algorithm. The other constants were known or could be assumed with sufficient certitude and therefore were not varied by the program. The optimal fit

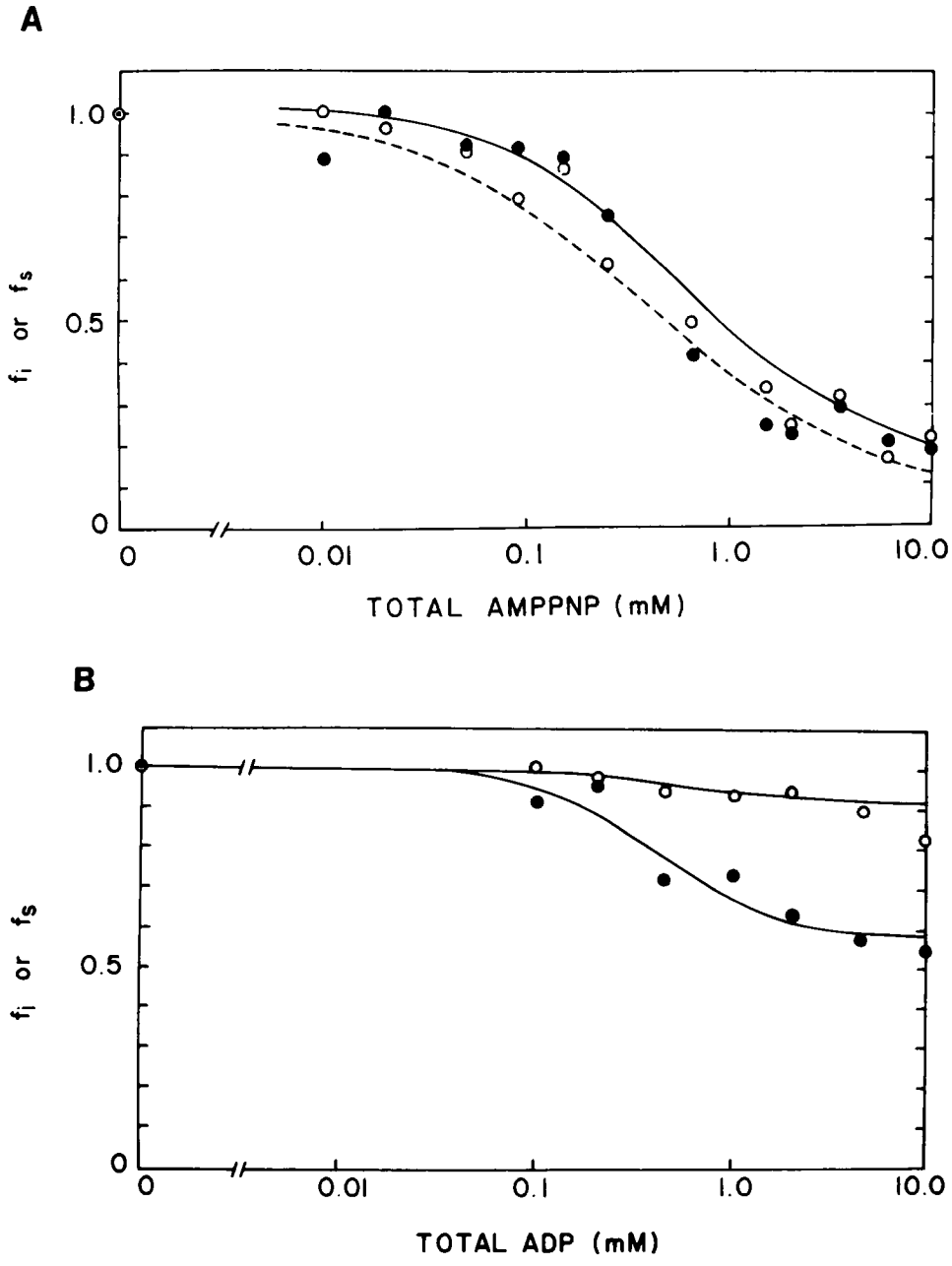

FIGURE 2 The dependence of the fraction of immobilized (f_i) or bound molecules (f_s) of MSL-HMM on the concentration of AMPPNP (*A*) or ADP (*B*) —●—, f_i measured by ST-EPR; ---○--- f_s measured by sedimentation. Spectra were obtained using solutions containing 9.35 μM (*A*) or 8.8 μM (*B*) MSL-HMM and 60 μM actin with other conditions given in the legend of Fig. 1. Curves were produced by computer modeling of the data using the scheme in Fig. 5 *A*.

was achieved by minimizing the sum of the squares of the difference between the calculated and experimental values of both f_s and f_i: error = $[(f_{scalc} - f_s)^2 + (f_{icalc} - f_i)^2]$. To compare the experimental and calculated values of f_i, we assumed that bound heads are immobilized and that free heads are not.

The total concentrations of MSL-HMM, actin and nucleotide (L_T) and initial guesses of the cumulative formation constants were used by an iterative procedure (23) to determine the free concentrations of nucleotide, MSL-HMM and actin. A separate determination of these concentrations was made for each value of L_T. With these values, the fractions of actin monomers occupied by MSL-HMM bound by one head (θ_1) or by both heads (θ_2) were calculated using equations based on a one dimensional Ising model of HMM binding to actin that takes into account the "parking" problem created by the fact that HMM has two heads (24).

$$\theta_1 = K'[\text{MSL-HMM}]/\text{ROOT} \qquad (1a)$$

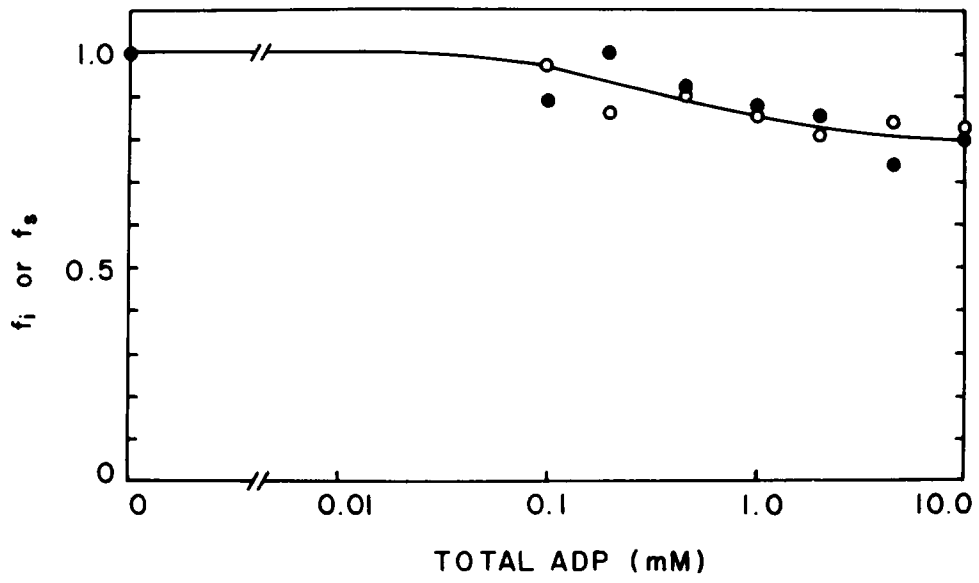

FIGURE 3 Dependence of the fraction of MSL-S1 bound to actin on the concentration of ADP. ●, f_i; ○, f_s. Actin, 60 μM; MSL-S1, 17 μM. The curve was obtained by computer modeling using the scheme shown in Fig. 5 *B*.

$$\theta_2 = 2K''[\text{MSL-HMM}]/\{(1 + K'[\text{MSL-HMM}] + \text{ROOT})\text{ROOT}\}, \quad (1b)$$

where $\text{ROOT} = \{(1 + K'[\text{MSL-HMM}])^2 + 4K''[\text{MSL-HMM}]\}^{1/2}$

and
$$K' = K_{AM} + K_{AML} \times L + K_{AML2} \times L^2 \quad (2a)$$

$$K'' = K_{A2M} + K_{A2ML2} \times L + K_{A2ML2} \times L^2, \quad (2b)$$

where L is the concentration of free nucleotide. The values of M_{1b} and M_{2b} (the total concentrations of all complexes with MSL-HMM bound by one or by both heads, respectively) are given by

$$M_{1b} = \theta_1 \times A_0 \quad (3a)$$

$$M_{2b} = \theta_2 \times A_0, \quad (3b)$$

where A_0 is the total actin concentration.

The calculated fractions are

$$f_{calc} = (M_{2b} + M_{1b})/\text{MSL-HMM}_{total} \quad (4a)$$

$$f_{calc} = (2M_{2b} + M_{1b})/2\text{MSL-HMM}_{total}. \quad (4b)$$

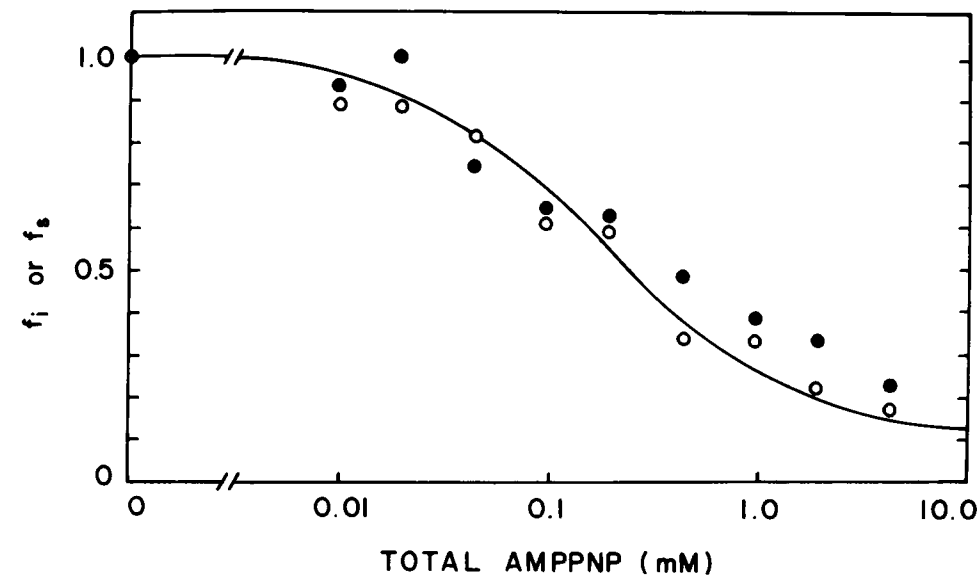

FIGURE 4 Dependence of the fraction of MSL-S1 bound to actin on the concentration of AMPNP. Actin, 60 μM; MSL-S1, 18 μM. ●, f_i; ○, f_s. The drawn curve was obtained from computer modeling using the scheme shown in Fig. 5 *B*.

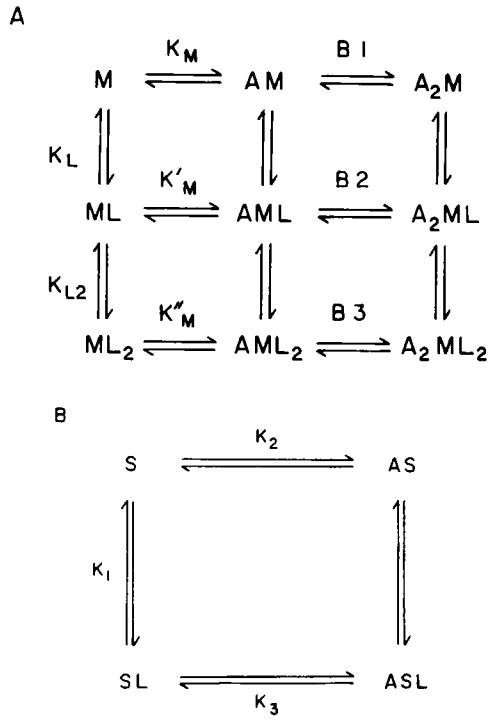

FIGURE 5 Binding scheme used in the analysis of the titration of acto-MSL-HMM (*A*) or acto-MSL-S1 (*B*) with nucleotide. A_iML_j represents a complex of actin (*A*) MSL-HMM (M) MSL-S1 (S) and nucleotide (L) where *i* and *j* can have values of 0, 1, or 2. Single- and double-headed binding of MSL-HMM to actin are indicated by values of $i = 1$ and 2, respectively. (*B*) Scheme for the analysis of the titration of acto-MSL-S1 with nucleotide where S represents MSL-S1.

Those cumulative formation constants that are not fixed are then readjusted to the fitting algorithm and the entire process is repeated until the error is at a minimum.

Acto-MSL-HMM + ADP

Five cumulative constants were fixed in fitting the titration data and these were estimated from experimental and literature data. Schaub and colleagues (25, 26) have suggested that nucleotide binds to one head of myosin much more weakly than to the other. To determine whether nucleotide binds to both heads of MSL-HMM with the same affinity, the binding of ϵADP to MSL-HMM was measured by fluorescence. Bound ϵADP was determined as described in Methods, and $[\epsilon ADP]_{free}$ was obtained by subtraction from $[\epsilon ADP]_{total}$. A plot of ΔF vs. the concentration of free ϵADP (not shown) could be described in terms of MSL-HMM having two equivalent binding sites for ϵADP. The best fit values of the binding constant and number of sites are $2 \times 10^5 M^{-1}$ and 2.3, respectively. Additional evidence was obtained in a separate experiment where MSL-HMM was digested with chymotrypsin in the presence of 20 μM ϵADP (see Methods). If ϵADP bound more weakly to one head, then digestion of MSL-HMM yielding two strongly binding molecules of MSL-S1 would almost double the fluorescence intensity. However, the fluorescence remained constant over a 90 min period, during which MSL-HMM was essentially completely converted to MSL-S1 as indicated by gel electrophoresis in sodium dodecyl sulfate. The results of these two experiments strongly suggest that ϵADP binds to both heads of MSL-HMM with equal strength, therefore in fitting the data to scheme 5A we assumed that the first and second nucleotides bind to MSL-HMM with the same intrinsic affinity. Thus, the binding constant (K_L) for the first ADP bound to MSL-HMM was twice that obtained from the titration with ϵADP, i.e. $K_L = 4 \times 10^5 M^{-1}$, while the second ADP binding constant, K_{L2}, equals one-half of this value; i.e., $1 \times 10^5 M$ and the formation constant for ML_2 ($K_{ML2} = K_L \times K_{L2})^{-1}$ has a value of $4 \times 10^{10} M^{-2}$.

For the binding of the first head to actin we assumed that the constants K_M, K'_M, K''_M could be estimated from the binding constants of MSL-S1; K_2 and K_3 (Fig. 5 *B*). Experimental data and theoretical considerations suggest that the first head of MSL-HMM binds to actin with a constant equal to that of MSL-S1 (27, 28); i.e., $K_M = K_2$ and $K''_M = K_3$. We assume $K'_M = 0.5\ K_M$ because only the head free of nucleotide contributes significantly to the binding.

The MSL-S1 binding constants K_2 and K_3 were determined in two experiments, the first being a titration of actin with MSL-S1 in the presence of excess ADP where all MSL-S1 was present as the complex ADP-MSL-S1 (Fig. 6). A Scatchard plot of $[MSL\text{-}S1]_{bound}/(actin \times [MSL\text{-}S1]_{free})$ vs. $[MSL\text{-}S1]_{bound}/actin$ has a slope of $8.3 \times 10^4 M^{-1}$, which in turn is equal to K_3 (22). The second was a titration of acto-MSL-S1 with ADP (Fig. 3). Here, the fitting program was used to find the optimal value for K_2 by using scheme 5b to model the data. K_3 was kept fixed at the previously determined value (see above) and K_1 was

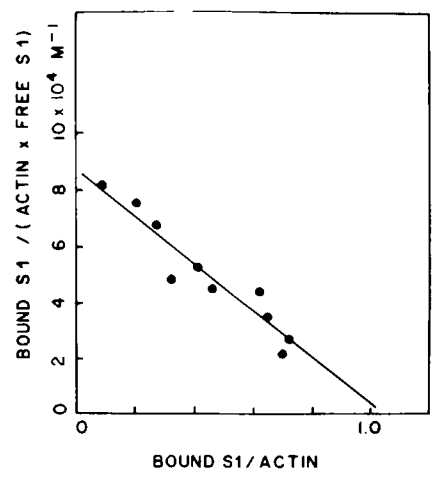

FIGURE 6 Titration of actin with ADP-MSL-S1. The slope is equal to K_3 of Fig. 5 *B*. The solution contained 3 mM ADP, 10 μM actin, 0.2 M KCl, 50 mM MOPS, 5 mM $MgCl_2$, 20 μM Ad_2P_5, pH 7. The concentration of MSL-S1 was varied from 0 to 40 μM.

TABLE I
BEST FIT CUMULATIVE BINDING CONSTANTS

Constant	ADP	AMPPNP
K_{ML}	$4.0 \times 10^5\ M^{-1}$	$4.0 \times 10^6\ M^{-1}$
K_{ML2}	$4.0 \times 10^{10}\ M^{-2}$	$4.0 \times 10^{12}\ M^{-2}$
K_{AM}	$8.5 \times 10^6\ M^{-1}$	$8.5 \times 10^6\ M^{-1}$
K_{AML}	$1.7 \times 10^{12}\ M^{-2}$	$1.7 \times 10^{13}\ M^{-2}$
K_{AML2}	$3.4 \times 10^{15}\ M^{-3}$	$1.2 \times 10^{16}\ M^{-3}$
K_{A2M}	$1.5 \times 10^9\ M^{-1}$	$1.5 \times 10^9\ M^{-1}$
K_{A2ML}	$3.6 \times 10^{12}\ M^{-2}$	$4.2 \times 10^{13}\ M^{-2}$
K_{A2ML2}	$1.2 \times 10^{15}\ M^{-3}$	$1.2 \times 10^{13}\ M^{-3}$

TABLE II
BINDING CONSTANTS OF FIRST AND SECOND HANDS

Constant		ADP	AMPPNP
K_M	$8.5 \times 10^6\ M^{-1}$		
K'_M		$4.3 \times 10^6\ M^{-1}$	$4.3 \times 10^6\ M^{-1}$
K''_M		$8.3 \times 10^4\ M^{-1}$	$3.1 \times 10^3\ M^{-1}$
$B1$*	180		
$B2$*		2.0	2.5
$B3$*		0.35	~0.001

*$B1 = K_{A2M}/K_{AM}$, $B2 = K_{A2ML}/K_{AML}$, $B3 = K_{A2ML2}/K_{A2ML}$.

fixed at the literature value of $2 \times 10^5 M^{-1}$ (29). The best fit value of K_2 is $8.5 \times 10^6 M^{-1}$.

With values of K_M, K'_M and K''_M in hand, estimates of the cumulative formation constants are then calculated as the product of the individual equilibrium constants leading up to that complex, viz. $K_{AM} = K_M$, $K_{AML} = K_L \times K'_M$ and $K_{AML2} = K_L \times K_{L2} \times K''_M$. The five constants ($K_{AM}$, K_{AML}, K_{AML2}, K_{ML}, K_{ML2}) were held fixed while K_{A2M}, K_{A2ML} and K_{A2ML2} were optimized. The resulting best fit values of these constants are given in Tables I and II. The calculated curves reproduced both f_s and f_i data quite well (Fig. 2 *B*).

The computer fitting results in a calculation of the concentration of each acto-HMM-nucleotide complex as a function of total concentration of ADP (Fig. 7). At ADP concentrations <0.3 mM, A_2M and A_2ML are the dominant complexes. Complexes in which MSL-HMM binds to actin by one head, AML and AML_2, are at very low concentrations. Above 0.3 mM ADP, the concentration of A_2M decreases sharply, while A_2ML reaches a maximum of 28% of the total MSL-HMM at 0.5 mM ADP. AML_2 dominates this part of the titration, reaching 60% of the total MSL-HMM. A_2ML_2, AML and AM are not major species at any point in the titration.

Acto-MSL-HMM + AMPPNP

The cumulative formation constants for the titration with AMPPNP were estimated as in the titration with ADP; values of $K_L = 2K_1 = 4 \times 10^6 M^{-1}$ and $K_{L2} = 1 \times 10^6 M^{-1}$ were obtained using the literature value of K_1 (29) and the same values for K_M, K'_M and B1 were used as in the ADP titration, because these steps describe the binding of a nucleotide-free head of MSL-HMM to actin. K_{AML} and K_{AML2} were obtained as described in section a. Since $K''_M = K_3$, K_3 was estimated by fitting the titration of acto-MSL-S1 with AMPPNP (Fig. 4) to scheme 5B with K_2 and K_1 fixed at $8.5 \times 10^6 M^{-1}$ (see section a) and $2 \times 10^6 M^{-1}$, respectively. A value of $3.1 \times 10^3 M^{-1}$ was obtained for K_3. Data from the acto-MSL-HMM titration were then fitted to obtain optimal values for K_{A2ML} and K_{A2ML2}, while all other formation constants remained fixed (Table I). The calculated curves for f_s and f_i agree with the measured values within the experimental error (Fig. 2 *A*).

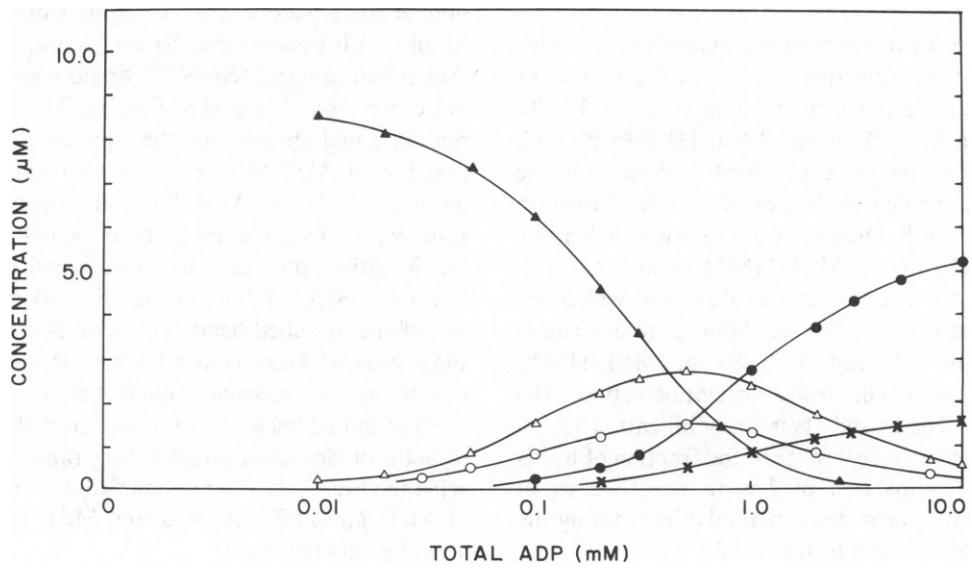

FIGURE 7 Concentration of the complexes A_iML_j as a function of the total concentration of ADP obtained from the best fit to the titration of acto-MSL-HMM with ADP (Fig. 2 *B*). Each sample contained 8.8 μM MSL-HMM. ▲, A_2M; O, AML; ●, AML_2; △, A_2ML; x, A_2ML_2.

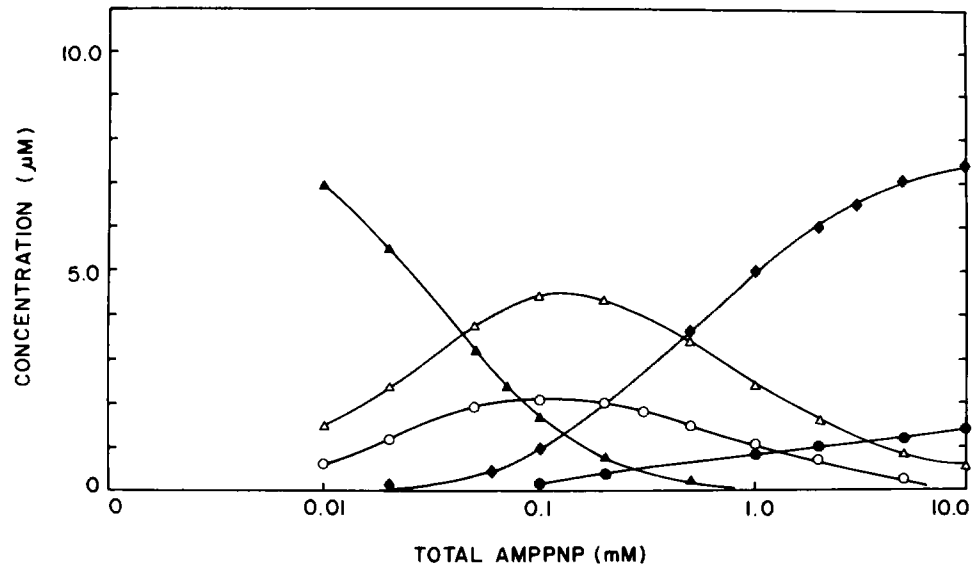

FIGURE 8 Concentration of the complexes A_iML_j as a function of the total concentration of AMPPNP obtained from the best fit to the titration of acto-MSL-HMM with AMPPNP (Fig. 2 *A*). Each sample contained 9.35 μM MSL-HMM. ▲, A_2M; O, AML; ●, AML_2; △, A_2ML; x, ML_2.

The distribution of complexes present during the titration with AMPPNP is shown in Fig. 8. In the first half of the titration, below 0.3 mM AMPPNP, A_2M decreases from 100 to 5%, while A_2ML and AML reach maxima of 50 and 23% of the total MSL-HMM, respectively. In contrast to the titration with ADP, almost complete dissociation of MSL-HMM from actin occurs in the latter half. Throughout the titration, the sum of the concentrations of single-headed complexes AML_2 and AML does not exceed 25% of the total MSL-HMM.

DISCUSSION

Saturation-transfer EPR spectroscopy in combination with rigid spin-labeling is a sensitive monitor of the motion of proteins in the submillisecond time domain (1, 3, 4, 19, 20, 30). By combining ST-EPR of acto-MSL-HMM with high speed centrifugation we have obtained evidence for the existence of single-headed binding of MSL-HMM to actin in the presence of ADP. During titrations with nucleotide, dissociation of MSL-S1 or MSL-HMM from actin produces changes in the rate of rotational motion which are reflected in the parameter L''/L, enabling us to determine the fraction of immobilized MSL-S1 or MSL-HMM heads, f_i (see Methods). The strong correlation between the fraction of bound heads and their immobilization (3, 5) permits f_i to be used as an estimate of the fraction of heads bound to actin. Comparison of f_i with the fraction of sedimented HMM, f_s, provides a method of estimating the fraction of molecules bound by one head.

On titration of acto-HMM with ADP, f_i decreased much more than did the fraction of bound molecules, f_s. We have considered two possible explanations for this observation, one being that a significant fraction of the MSL-HMM binds by only one head, the bound head being immobilized while the unbound head rotates freely. This would decrease f_i but would not change f_s because the mobile heads sediment with actin, being attached through their bound partner. Another explanation is that all MSL-HMM is bound by both heads, but when at least one head carries ADP both rotate at an intermediate rate—between those of free and immobilized heads—accounting for the decrease in L''/L and f_i (1, 3).

The fact that f_i and f_s decrease in parallel on titration of MSL-S1 with ADP argues against the second interpretation. If there were a ternary complex of acto-ADP-MSL-S1 in which bound MSL-S1 had more motional freedom than it had in acto-MSL-S1, f_i would become less than f_s as more such complexes were formed. The fact that f_s and f_i remain equal throughout the titration (Fig. 3) indicates that bound ADP-MSL-S1 does not have a faster rate of motion than bound MSL-S1. This suggests that a bound state with increased mobility does not exist for MSL-HMM either, provided that the absence of an intact light chain 2 in S1 (31) does not significantly affect the properties of the attached head. This idea is consistent with the suggestion of Thomas and Cooke (4) and Ishiwata et al. (5) that in the presence of nucleotide, the heads of myosin are distributed between two states: immobilized by binding to actin or detached and rotating rapidly. The data fit a scheme (Fig. 5 *A*) where, depending on the concentration of ADP, up to 60% of the bound MSL-HMM attaches to actin by only one head.

Computer fitting of the data to the model in Fig. 5 *A* yielded information on the extent of single-headed vs. double-headed binding of MSL-HMM to actin in rigor

and in the presence of nucleotides. In rigor there is no single-headed binding because B1 = $[A_2M]/[AM]$ = 180, this value being of the same order of magnitude as previously measured (10, 28, 29). In the presence of nucleotide, the extent of single-headed binding is governed not only by B1, B2, and B3, but also by the other constants. In the titration, at lower concentrations of ADP, the binding of one ADP to MSL-HMM (ML complex) reduces the affinity of the second head for actin (B2 = 2) resulting in the concentration of A_2ML being greater than that of AML throughout the titration (Fig. 7). As the concentration of ADP increases above 0.3 mM, both heads become occupied by ADP (ML_2) and because B3 = 0.35, single-headed binding predominates (Fig. 7).

Saturation of MSL-HMM with ADP reduces the binding constant of the first head to actin by a factor of 100 (K''_M vs. K_M), while that of the second head is reduced by a factor of 500 (B3 vs. B1). The larger effect of nucleotide on the binding of the second head suggests that ADP renders the structural changes, presumably taking place when the second head binds to actin (27), less favorable. It should be noted that the effect of the bound nucleotide on the binding constants of each of the two heads is not considered as evidence for cooperatively between the heads with respect to nucleotide binding in unattached MSL-HMM or myosin. A simpler explanation for the effect involves some sort of distortion as the second head binds. Our results with ϵADP furnish no evidence for head-head interactions in ligand binding such as those suggested by Schaub and colleagues (25, 26). In titrations of MSL-HMM we found no support for a difference in binding of ϵADP to the two heads.

When AMPPNP is the titrant f_s and f_i are equal within experimental error (Fig. 2 A). The reason for the dissimilar results of the ADP and AMPPNP titrations can be found by examining the difference $\Delta f = f_{scalc} - f_{icalc} = M_{1b}/[\text{heads}]_{total}$ obtained by subtracting Eq. 4b from Eq. 4a. At concentrations of AMPPNP <0.2 mM, the computer fitting of the titration data showed that the only single-headed complex present is AML (Fig. 8) and that its concentration, ~2 μM, is small compared to that of the heads (~18 μM) so that Δf has a value of ~0.11. When the concentration of AMPPNP is greater than 0.2 mM, the concentration of AML is reduced further and the most populated species containing two bound ligands becomes ML_2 (Fig. 8), resulting again in a value of Δf that is <0.1—the experimental error in the measurement of f_i and f_s. In the case of ADP, the dominant species is AML_2, yielding Δf of 0.1 to 0.35. Therefore only ADP produces a difference between f_i and f_s that is large enough to be detected by our methods.

Previous work (10) on the binding of HMM to actin indicated that K_{A2M} was $3 \times 10^9 M^{-1}$ (μ = 0.22 M), in good agreement with our result of $1.5 \times 10^9 M^{-1}$, while their estimate of B1 is a factor of only 3 larger than ours. Greene (10) also measured the equilibrium constant of the second head (B3) in the presence of 4 mM ADP (μ = 0.43 M) or 4 mM AMPPNP (μ = 0.12 M) and found a value of 2–5 in both cases. She concluded that the second head of HMM binds weakly in the presence of ADP and possibly not at all in the presence of AMPPNP. Our value of B3 shows that at μ = 0.2M the second head does not bind at saturating concentrations of ADP. However, our results cannot be compared directly with those of Greene because of nonidentical experimental conditions. Chen and Reisler (12) have also recently found, in agreement with our results, that single-headed binding of HMM to actin is detectable in the presence of ADP but not in the presence of AMPPNP. The work of Hackney and Clark (11) suggests that single-headed binding of HMM to actin occurs in the presence of very low concentrations of ATP. Our results with ADP differ in that single-headed binding occurs to the greatest extent at the higher concentrations of ADP, where both heads carry the nucleotide. A possible explanation is that ATP, or its bound breakdown products, weakens the binding of the HMM heads much more than does ADP alone so that the species $actin_2$-HMM-ATP, $actin_2$-HMM-ATP_2 and actin-HMM-ATP_2 form in undetectable quantities.

The demonstration of the presence of a substantial fraction of ADP-MSL-HMM attached to actin by a single head is of interest in the light of the work of Burghardt et al. (9); the dichroism of a rhodamine derivative attached to the reactive SH1 thiol group of myosin in glycerol extracted muscle fibers indicated that the orientation of attached heads in the presence of ADP or in contracting fibers was different from that of rigor. At present, it is not clear whether or not these data are related to single-headed attachment of myosin, nor is it clear how the implications of single-headed binding may affect current models of the contraction cycle.

This work was supported by grants HL-5949, HL-15391, and HL-7226 from the National Institutes of Health and by grants from the National Science Foundation and the Muscular Dystrophy Association.

Received for publication 13 September 1985 and in final form 17 February 1986.

REFERENCES

1. Thomas, D. D., J. C. Seidel, J. S. Hyde, and J. Gergely. 1975. Motion of subfragment-1 in myosin and its supramolecular complex: saturation transfer electron paramagnetic resonance. *Proc. Natl. Acad. Sci. USA.* 72:1729–1733.
2. Seidel, J. C. 1973. The effects of actin on the electron spin resonance of spin labeled myosin. *Arch. Biochem. Biophys.* 157:588–596.
3. Thomas, D. D., S. Ishiwata, J. C. Seidel, and J. Gergely. 1980. Submillisecond rotational dynamics of spin-labeled myosin heads in myofibrils. *Biophys. J.* 32:873–889.
4. Thomas, D. D., and R. Cooke. 1980. Orientation of spin-labeled myosin heads in glycerinated muscle fibers. *Biophys. J.* 32:891–906.
5. Ishiwata S., B. A. Manuck, J. C. Seidel, and J. Gergely. 1985. Saturation transfer electron paramagnetic resonance studies of attachment of myosin heads in myofibrils. *Biophys. J.* 49:821–829.

6. Nagano, H., and Yanagida, T. 1984. Predominant attached state of myosin cross-bridges during contraction and relaxation at low ionic strength. *J. Mol. Biol.* 177:769–785.
7. Huxley, H. E., R. M. Simmons, A. R. Farqui, M. Kress, J. Bordas, and M. H. J. Koch. 1983. Changes in the X-ray reflections from contracting muscle during rapid mechanical transients and their structural implications. *J. Mol. Biol.* 169:469–506.
8. Huxley, H. E., and M. Kress. 1985. Crossbridge behaviour during muscle contraction. *J. Muscle Res. Cell Motil.* 6:153–161.
9. Burghardt, T. P., T. Ando, and J. Borejdo. 1983. Evidence for crossbridge order in contraction of glycerinated skeletal muscle. *Proc. Natl. Acad. Sci. USA.* 80:7515–7519.
10. Greene, L. E. 1981. Comparison of the binding of heavy meromyosin and myosin subfragment 1 to F-actin. *Biochemistry.* 20:2120–2126.
11. Hackney, D. D., and P. K. Clark. 1984. Catalytic consequences of oligomeric organization: kinetic evidence for "tethered" actoheavy meromyosin at low ATP concentrations. *Proc. Natl. Acad. Sci. USA.* 81:5345–5349.
12. Chen, T., and E. Reisler. 1984. Tryptic digestion of rabbit skeletal myofibrils: an enzymatic probe of myosin crossbridges. *Biochemistry.* 23:2400–2407.
13. Eads, T., D. D. Thomas, and R. Austin. 1984. Microsecond rotational motions of eosin-labeled myosin measured by time-resolved anisotropy of absorption and phosphorescence. *J. Mol. Biol.* 179:55–81.
14. Kinosita, K., S. Ishiwata, H. Yoshimura, H. Asai, and A. Ikegami. 1984. Submicrosecond and microsecond rotational motions of myosin heads in solution and in myosin synthetic filaments as revealed by time-resolved optical decay measurements. *Biochemistry.* 23:5963–5975.
15. Mendelsohn, R. A., M. F. Morales, and J. Botts. 1973. Segmental flexibility of the S-1 moiety of myosin. *Biochemistry.* 12:2250–2255.
16. Nauss, K., S. Kitagawa, and J. Gergely. 1969. Pyrophosphate binding to and adenosine triphosphatase activity of myosin and its proteolytic fragments. *J. Biol. Chem.* 244:755–765.
17. Weeds, A. G., and B. Pope. 1977. Studies on the chymotryptic digestion of myosin. Effects of divalent cations on proteolytic susceptibility. *J. Mol. Biol.* 111:129–157.
18. Graceffa, P., and J. C. Seidel. 1980. A reaction involving protein sulfhydryl groups, a bound spin-label and $K_3Fe(CN)_6$ as a probe of sulfhydryl proximity in myosin. *Biochemistry.* 19:33–39.
19. Thomas D. D., J. C. Seidel, and J. Gergely. 1979. Rotational dynamics of spin-labeled F-actin in the sub-millisecond time range. *J. Mol. Biol.* 132:257–273.
20. Thomas, D. D., L. R. Dalton, and J. S. Hyde. 1976. Rotational diffusion studied by passage saturation transfer EPR. *J. Chem. Phys.* 65:3006–3024.
21. Ando, T., J. Duke, Y. Tonomura, and M. F. Morales. 1982. Spectroscopic isolation of complexes of myosin subfragment-1 ATPase by fluorescence quenching. *Biochem. Biophys. Res. Commun.* 109:1–6.
22. Greene, L. E., and E. Eisenberg. 1978. Formation of a ternary complex: actin, 5'-adenylyl imidodiphosphate and the subfragments of myosin. *Proc. Natl. Acad. Sci. USA.* 75:54–58.
23. Perrin, D. D., and I. G. Sayce. 1967. Computer calculation of equilibrium concentrations in mixtures of metal ions and complexing species. *Talanta.* 14:833–842.
24. Hill, T. L. 1978. Binding of monovalent and divalent myosin fragments onto sites on actin. *Nature (Lond.).* 274:825–826.
25. Schaub, M. C., and J. G. Watterson. 1981. Symmetry and asymmetry in the contractile protein myosin. *Biochimie.* 63:291–299.
26. Kunz, P. A., K. Loth, J. G. Watterson, and M. C. Schaub. 1980. Nucleotide induced head-head interaction in myosin. *J. Muscle Res. Cell Motil.* 1:15–30.
27. Hill, T. L., and E. Eisenberg. 1980. Theoretical considerations in the equilibrium binding of myosin fragments on F-actin. *Biophys. Chem.* 11:271–281.
28. Greene, L. E., and E. Eisenberg. 1980. The binding of heavy meromyosin to F-actin. *J. Biol. Chem.* 255:549–554.
29. Greene, L. E., and E. Eisenberg. 1980. Dissociation of the actin subfragment-1 complex by adenyl-5'-yl imidodiphosphate, ADP and PP_i. *J. Biol. Chem.* 255:543–548.
30. Thomas, D. D., J. C. Seidel, and J. Gergely. 1976. Molecular motions and the mechanism of muscle contraction and its regulation. *In* Contractile Systems in Non-muscle Tissue. S. V. Perry, et al., editors. Elsevier, North Holland. pp. 13–21.
31. Weeds, A. G., and R. S. Taylor. 1975. Separation of subfragment 1 isoenzymes from rabbit skeletal muscle myosin. *Nature (Lond.).* 257:54–56.